Influence of cross-linking on the segmental dynamics in model polymer networks

V. Yu Kramarenko,[a] T. A. Ezquerra,[b] I. Šics,[c] and F. J. Baltá-Calleja
Instituto de Estructura de la Materia, C.S.I.C. Serrano 119, Madrid 28006, Spain

V. P. Privalko
Institute of Macromolecular Chemistry, National Academy of Sciences of Ukraine, 253160 Kyiv, Ukraine

In an attempt to study the specific influence of cross-linking on the α relaxation in polymer networks, a series of model heterocyclic polymer networks (HPN) with well-defined cross-link densities and constant concentration of dipolar units were studied. Model HPN systems were prepared by simultaneous trimerization of 1,6-hexamethylene diisocyanate (HMDI) and hexyl isocyanate (HI). These HPN systems were characterized by dielectric relaxation spectroscopy in the $10^{-1}\,\mathrm{Hz} < F < 10^{5}\,\mathrm{Hz}$ frequency range and in the $123\,\mathrm{K} < T < 493\,\mathrm{K}$ temperature interval. The α relaxation in these systems depends on network density and shifts toward higher temperatures as the cross-link density increases for high HMDI/HI ratios. Discussion of the α-relaxation shape in light of recent models indicates that segmental motions above the glass transition systematically experience a growing hindrance with increasing degree of cross-linking. Description of the temperature dependence of relaxation times according to the strong–fragile scheme clearly shows that fragility increases as polymer network develops. © 2000 American Institute of Physics. [S0021-9606(00)50724-7]

I. INTRODUCTION

The onset of liquidlike mobility in glass forming systems at the length scale of relevant molecular units is a characteristic feature of the glass transition. In polymeric systems, provided that the molecular weight is high enough, long time dynamics is controlled by topological constraints called entanglements.[1] This effect forces the large-scale conformational dynamics to occur by diffusion (reptation) within a tube.[1–4] At length scales shorter than the average distance between entanglements, the dynamics proceeds through normal modes and it is assumed to be similar for both entangled and nonentangled polymers. An analogous similarity is expected at the length scale of few polymer segments, where normal mode dynamics crosses over to segmental relaxation, giving rise to the α relaxation. In many respects, entanglements in linear polymers play a similar role as cross-links in a polymer network. The influence of network formation on the relaxation behavior of polymer networks is an issue of considerable experimental effort.[5–7] Comparison between the dynamic behavior of a covalently entangled and cross-linked polymer, with low volume fraction of cross-links, has shown similar features in both the normal mode and the segmental relaxation regime.[8] However, previous studies have shown a strong influence of cross-link density on the α relaxation characterized by a slowing down of the segmental dynamics as cross-links density, inducing connectivity, increases.[9,10] In many studies, the true impact of chemical network density is obscured by several side effects such as morphological heterogeneity and strong physical interaction in segmented polyurethanes,[7] incomplete chemical conversion in acrylates,[6] or anomalous chain flexibility of network strands in polysiloxanes.[5] Some of these side effects can be minimized by controlled preparation of model polymer networks with well-defined molecular architecture. It is known that the appropriate trimerization of isocyanate in the presence of tin compounds produces a regular isocyanourate network.[11,12] Copolymers consisting of three-arm (cross-linked) and two-arm (linear) segments can be obtained in the case of simultaneous trimerization of mono- and di-isocyanates.[13–15]

In the present work we have synthesized and studied the dynamical properties of a series of well-defined heterocyclic polymer networks (HPN) with a controlled ratio of trimerized mono- and di-isocyanates which can be envisioned as HPN models. An important feature of these systems is an almost invariant concentration of dielectrically active components in spite of the significant topology variation. The aim of this study is to investigate the influence of the cross-link's density on the α relaxation of these model polymer networks.

II. EXPERIMENTAL PART

A. Materials

Simultaneous trimerization reaction of 1,6-hexamethylene diisocyanate (HMDI) and hexyl isocyanate (HI) was accomplished by mixing of carefully weighed and vigorous stirring (3–5 min) of the two reaction components and catalyst (hexa-*n*-butyldistannum oxide). Initial ratios of mix-

[a]Permanent address: Kharkov State Polytechnical University, 310002, Frunze 21, Kharkov, Ukraine.
[b]Electronic mail: imtel55@iem.cfmac.csic.es
[c]Permanent address: Riga Technical University, Institute of Polymer Materials, Latvia.

TABLE I. Parameters of the investigated systems: HMDI/HI initial molar ratio, (L/N) relative ratio of linear to network content, (M_c) average molecular weight of segment between cross-links, and (P) content of NCO polar groups.

HMDI/HI	L/N	M_c (g/mol)	$P(\%)$
1:1	100/0	$\cdots$	42.7
1.5:1	75/25	1137.0	44.3
2:1	60/40	694.5	45.4
3:1	43/57	473.3	46.6
1:0	0/100	252	50

ture components are presented in Table I. The reaction mixture was stored under isothermal conditions ($T = 373$ K) during 12–16 hours, cooled back to room temperature, and then placed into a space between two parallel, specially treated glass plates of sample cell. The loaded cell was again heated to 373 K and isothermally stored. After the total storage time of 38 h, a polymer sample was stripped off and evacuated at 373 K to remove all traces of residual monomers from plate surfaces. Finally, the cure of each polymer sample was completed by slow heating to 443 K (for all HMDI/HI ratios) or to 493 K (for a pure HMDI) and isothermally stored during 2.5 h. By this procedure a regularly cross-linked copolymer is obtained with precise molar fractions of three-arm (cross-linked) and of two-arm (linear) segments (Fig. 1). Assuming a full conversion of the reacting groups and formation of a defect-free network structure some relevant structural parameters can be calculated (Table I). Here, L/N refers to relative ratio of linear to network structure (Fig. 1), M_c average molecular weight of chain segment enclosed between two cross-links, and P is molar content of NCO groups in the copolymers.

In order to perform dielectric measurements, free polymer films (thickness 0.15–0.18 mm) were prepared in this fashion and coated with golden electrodes (diameter 20 mm) using a sputtering technique.

B. Techniques

Thermal analysis of the samples was carried out by differential scanning calorimetry (DSC), using a Perkin-Elmer DSC7 device at a heating rate of 10 K/min under nitrogen. The temperature was calibrated using Indium standards.

Complex dielectric permittivity, $\epsilon^* = \epsilon' - i\epsilon''$, was measured covering a frequency range 10^{-1} Hz$<$F$<10^5$ Hz by using an Standford lock-in amplifier SR830 with a dielectric interphase and control temperature unit from Novocontrol. Both shape and temperature evolution of the α relaxation
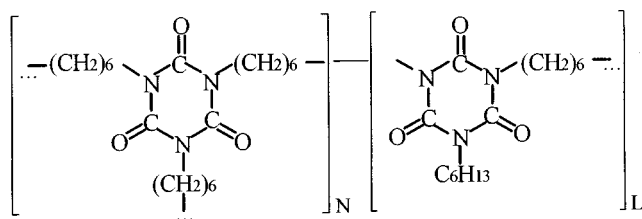

FIG. 1. Generalized chemical scheme of the heterocyclic copolymer network (HPN).

were analyzed as described elsewhere[16,17] by the phenomenological Havriliak–Negami (HN) description including a conductivity term.[18,19] According to this approach, the dielectric permittivity, ϵ^*, exhibits a frequency dependence of the type

$$\epsilon^* = \frac{\epsilon_0 - \epsilon_\infty}{[1 + (i\omega\tau_{HN})^b]^c} + \epsilon_\infty - i\frac{\sigma}{\epsilon_{vac}\omega^s}, \quad (1)$$

where $\omega = 2\pi F$, ϵ_0 and ϵ_∞ are the relaxed ($\omega = 0$) and unrelaxed ($\omega = \infty$) dielectric constant values, τ_{HN} is the central relaxation time of the relaxation time distribution function, and b and c ($0 < b, c < 1$) are shape parameters which describe the symmetric and asymmetric broadening of the relaxation time distribution function, respectively.[18] Here, σ is related to the direct current electrical conductivity, ϵ_{vac} is the vacuum dielectric constant, and s depends on the nature of the conduction mechanism. A value of $s < 1$ is associated with a non-ohmic transport.[19]

III. RESULTS

Dielectric loss, $\epsilon''(F)$, and dielectric constant data, $\epsilon'(F)$, measured in the available frequency window for five samples with different L/N molar ratios, are shown as a function of the frequency for different temperatures in Figs. 2 and 3, respectively. In all cases, ϵ'' measurements were taken at $T > T_g$ in order to focus on the α-relaxation process. As expected, the α relaxation manifests itself, for all systems, as a maximum in $\epsilon''(F)$. As the temperature increases, the frequency of maximum loss, F_{max}, shifts toward higher values. At low frequencies the relaxation is accompanied by a strong increase of $\epsilon''(F)$. Measurements extended to higher temperatures reveal that this effect corresponds to a direct current (dc)-conductivity contribution. The α relaxation appears as a step in the dielectric constant measurements.

At each temperature, ϵ'' and ϵ' values were fitted according to Eq. (1) and the result of this treatment is presented in Figs. 2 and 3 by the continuous curves. The separate contributions of both the relaxation and the conduction process have been also represented for ϵ''. The characteristic parameters of Eq. (1) such as $\Delta\epsilon = \epsilon_0 - \epsilon_\infty$, ϵ_0, b, c, τ_{HN}, σ, and s are obtained. Table II shows these parameters for temperatures of Fig. 2.

From the fitting parameters the value of $\tau_{max} = (2\pi F_{max})^{-1}$, where F_{max} is the frequency of maximum loss, can be obtained by[20]

$$\tau_{max} = \tau_{HN}\sin^{-1/b}(b\pi/(2+2c))\sin^{1/b}(bc\pi/(2+2c)). \quad (2)$$

The corresponding values for τ_{max}, shown in Fig. 4, reveal the Vogel–Fulcher–Tamann (VFT) dependence of τ_{max} with the reciprocal temperature as

$$\tau_{max} = \tau_0\exp\left(\frac{B}{T - T_0}\right). \quad (3)$$

To reduce the effect of data fitting to the VFT equation over a limited frequency range, a value of $\log_{10}\tau_0 \approx 14$ was assumed according to a recent proposal.[21] This assumption
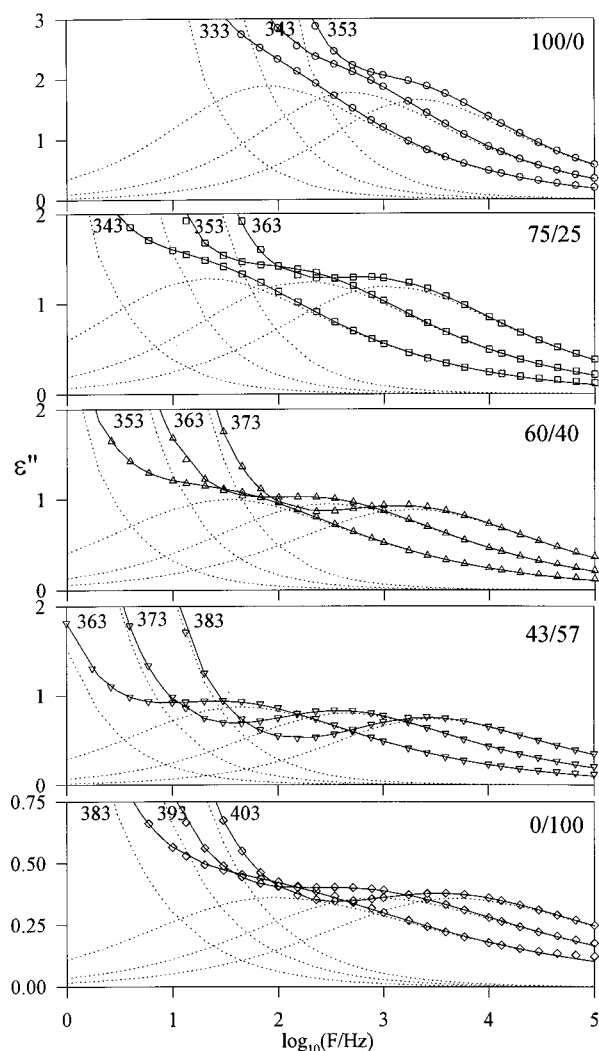
FIG. 2. Dielectric loss, ϵ'', for HPN systems with varying L/N ratios as a function of frequency at different temperatures for the α-relaxation process. The continuous lines represent the best fits to the HN relaxation function including the conductivity contribution.

FIG. 3. Dielectric constant, ϵ', for HPN systems with varying L/N ratios as a function of frequency at different temperatures for the α-relaxation process. The dotted lines represent the best fits to the HN relaxation function. The continuous lines are here as a guide for the eye.

does not affect the quality of the data fit into the VFT equation but reduces the dispersion among fitting parameters (Table III). Several schemes have been proposed to classify the degree of relaxation time departure from Arrhenius behavior at the α-relaxation process.[22–24] The strong–fragile scheme proposed by Angell[22] allows one to classify glass-forming systems on the basis of the temperature dependence exhibited by the relaxation time. Within this scheme, the fragility of a system has been defined by the degree of departure from the Arrhenius behavior exhibited by the relaxation time of the α-relaxation process.[22–24] Originally, the strength parameter, $D=B/T_0$, was introduced to characterize the fragility. Additionally, the steepness index $M = BT^*(T^* - T_0)^{-2}$ with $\tau_{\max}(T^*) = 10^2 s$ was also proposed to quantify fragility.[24] More recently, the parameter $F_{1/2} = (2T^*/T_{1/2}) - 1$ with $\tau_{\max}(T_{1/2}) = 10^6 s$ was derived.[20] In our case, for the sake of comparison, the corresponding values of the above-mentioned parameters are shown in Table III.
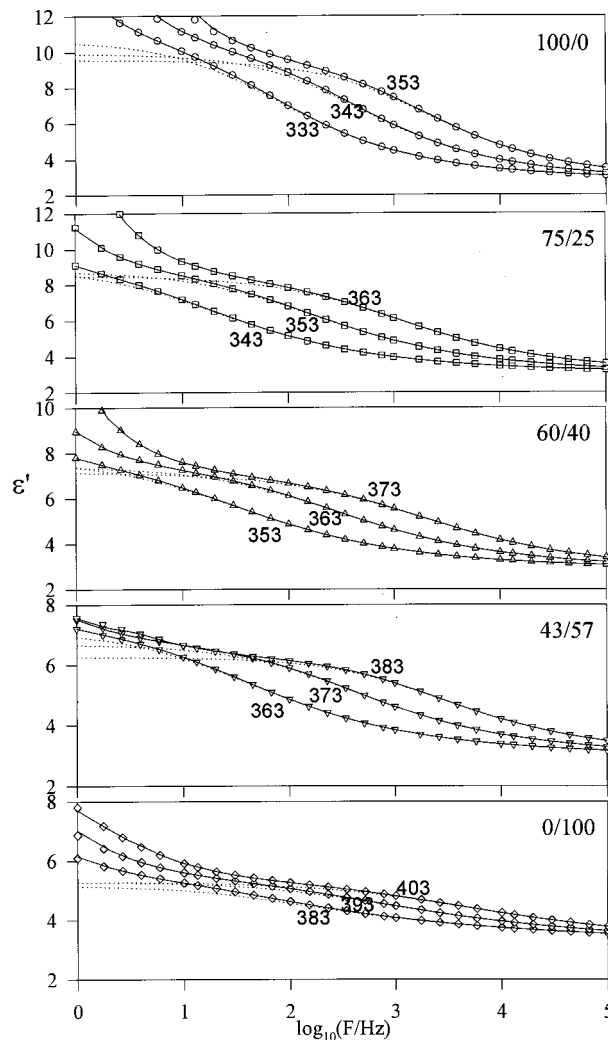
IV. DISCUSSION

A. Relationship between shape parameters and network connectivity

Schönhals and Schlosser have proposed a phenomenological model in which the shape parameters, which characterize the dielectric α relaxation in the frequency domain, can be related to the molecular dynamics at the glass transition provided that the molecular mobility is controlled by inter- and intramolecular interactions.[25] In this model, the b and c HN parameters are related to two new, so-called scaling parameters of the α-relaxation m and n by $m=b$ and $n = b \cdot c$. This model relates m to large-scale motions while n is controlled by small-scale motions. Experimental support of the model has been provided by different dielectric spectroscopy techniques.[26]

In our case, the $\Delta\epsilon$, m, and n parameters are shown in Fig. 5 for the investigated HPN systems as a function of the reciprocal temperature. The dielectric strength, $\Delta\epsilon$, increases linearly with the reciprocal temperature in all cases. In order

TABLE II. HN parameters of α relaxation of HPN.

L/N	T, K	$\Delta\epsilon$	ϵ_0	b	c	τ_{HN} (s)	σ (S/cm)	s
	333	8.04	10.807	0.638	0.688	$3.41*10^{-3}$	$1.41*10^{-10}$	0.93
100/0	343	7.25	10.076	0.665	0.670	$5.84*10^{-4}$	$4.96*10^{-10}$	0.88
	353	6.66	9.463	0.671	0.682	$1.27*10^{-5}$	$9.86*10^{-10}$	0.84
	343	5.86	8.947	0.629	0.598	$1.53*10^{-2}$	$1.19*10^{-10}$	0.93
75/25	353	5.68	8.752	0.618	0.632	$1.74*10^{-3}$	$5.01*10^{-10}$	0.94
	363	5.40	8.465	0.607	0.663	$2.65*10^{-4}$	$1.70*10^{-9}$	0.93
	353	4.87	7.786	0.575	0.649	$9.81*10^{-3}$	$1.10*10^{-10}$	0.88
60/40	363	4.55	7.452	0.569	0.692	$9.84*10^{-4}$	$4.50*10^{-10}$	0.89
	373	4.19	7.079	0.567	0.736	$1.44*10^{-4}$	$1.38*10^{-9}$	0.89
	363	4.22	7.245	0.577	0.655	$7.34*10^{-3}$	$6.85*10^{-11}$	0.89
43/57	373	3.71	6.659	0.605	0.646	$7.03*10^{-4}$	$2.47*10^{-10}$	0.88
	383	3.31	6.294	0.615	0.668	$1.12*10^{-4}$	$6.78*10^{-10}$	0.88
	383	2.35	5.685	0.598	0.406	$6.04*10^{-3}$	$4.59*10^{-11}$	0.67
0/100	393	2.15	5.456	0.571	0.452	$6.76*10^{-4}$	$9.52*10^{-10}$	0.67
	403	2.05	5.307	0.531	0.522	$1.02*10^{-5}$	$1.82*10^{-10}$	0.68

to discuss this temperature dependence one has to consider the Frölich–Kirwood (FK) equation[27] which describes the temperature dependence of the reduced dielectric strength $f(\epsilon_0)$ as

$$f(\epsilon_0) = \frac{(\epsilon_0 - \epsilon_\infty)(2\epsilon_0 + \epsilon_\infty)}{\epsilon_0(\epsilon_\infty + 2)^2} = \frac{4\pi\rho N_a}{9kTM}g\mu^2, \qquad (4)$$

where ρ is the density, μ is the dipole moment of the relaxing unit, M is the molecular weight of the repeating unit, N_a is Avogadro's number, and k is the Boltzmann constant. For our systems $f(\epsilon_0)$ [Fig. 5(b)], calculated according to the fitting parameters, increases linearly with reciprocal temperature as qualitatively expected according to the FK equation. As discussed in Ref. 5, the different slopes in Fig. 5(b) are the result of the temperature dependence of the different factor included in the right term of the FK equation. For fixed temperatures, the observed decrease of $f(\epsilon_0)$ with increasing cross-links density can be attributed, in a first approach, to the expected increase of intramolecular correlation upon going from 100/0 to 0/100. This effect would tend to reduce the correlation factor g.[28] A qualitatively similar effect has been reported to appear in crystallizable linear polymers as crystallinity develops and crystalline domains act as physical cross-links.[29] This reduction of the g-factor could also contribute, in a first approach, to the decrease of the slopes of $f(\epsilon_0)$ upon going from 100/0 to 0/100. A quantitative precise description of the $f(\epsilon_0)$ temperature dependence would require more extended theoretical calculations.[5,28]

The scaling parameters m and n exhibit a clear dependence on a cross-link's density decreasing upon going from 100/0 to 0/100. In order to visualize this effect, m and n values have been represented in Fig. 6 as a function of the molar ratio of the linear component. According to the model, an m decrease with cross-linking is expected to be due to the increase of intermolecular correlation.[7] As regards the n values, the observed decrease with growth in cross-linking indicates an increasing hindering of intrachain diffusion processes. These results are in agreement with previous investigations in systems, during polymer network formation,[30] where a decrease in both m and n was also observed. It is noteworthy that while m monotonically de-

creases with the cross-link's density in the whole molar ratio range, a clear decrease of n is only observed for the higher degree of cross-linking. This is in accordance with previous investigations in networks based on styrene-butyl acrylate divinylbenzene with a moderate degree of cross-linking in which n was not affected.[10]

B. Dependence of cooperativity on the cross-link's density

There is an evident dependence of the T_0 and D with the cross-link's density which is a reflection of the increase of T_g as the amount of cross-links increases (Table III). As shown in Fig. 4, τ_{max} values can be described by the VFT equation. Angell has proposed that fragility is connected with the to-
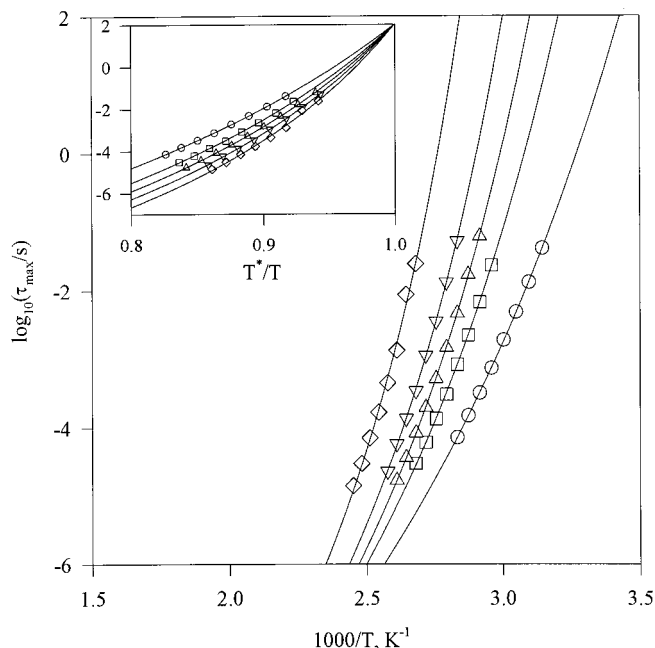

FIG. 4. τ_{max} values as a function of the reciprocal temperature for the HPN systems with different L/N ratios: 100/0○, 75/25□, 60/40△, 43/57▽, and 0/100◇. Inset shows same data in a cooperativity plot fashion [log τ_{max} vs T^*/T where $\tau_{max}(T^*)=10^2$ s]. Solid line is the corresponding VFT fittings.

TABLE III. T_g, VFT parameters, and stretching exponent for the HPN networks with different L/N ratio.

L/N	T_g (K)	τ_0 (s)	B	T_0 (K)	D	T^* (K)	$F_{1/2}$	m	β_{KWW}
100/0	287.6	$1*10^{-14}$	3632	193.0	18.82	291.6	0.49	109	0.43
75/25	310.1	$1*10^{-14}$	3256	223.5	14.57	311.9	0.56	130	0.39
60/40	324.6	$1*10^{-14}$	3044	239.7	12.70	322.3	0.59	144	0.37
43/57	337.1	$1*10^{-14}$	2864	255.3	11.22	333.0	0.62	158	0.37
0/100	362.0	$1*10^{-14}$	2746	276.8	9.92	351.3	0.65	174	0.29

pology of the potential energy associated with the available configurations. Upon increasing temperature throughout T_g, the latter are supposed to be modified, giving access to a different set of configurational states. In a different approach, Ngai et al.[23] associated fragility with the strength of the correlation between nonbonded species which these authors related to the cooperativity of the motion. In order to discuss the dependence of cooperativity with network density, τ_{max} data have been represented as a cooperativity plot (inset in Fig. 4). Here $\log_{10} \tau_{max}$ is represented as a function of a

normalized T^*/T parameter by taking T^* as the temperature at which the average relaxation time, defined as $\tau_{max} = (2 \cdot \pi \cdot F_{max})^{-1}$, equals 100 sec (see Ref. 20). From this representation it becomes clear that fragility or cooperativity, characterized in this plot by the slope at $T^*/T \rightarrow 1$, increases as network density increases. This effect correlates either with the decrease of D or with the increase of the M and $F_{1/2}$ parameters with increasing cross-linking (see Table III). Hence, this indicates that polymeric systems having similar chemical structure but a different degree of cross-linking exhibit, above T_g, very different dynamic features in terms of cooperativity. This is due to the inherent constraints to the segmental motions imposed by the cross-links.

A similar conclusion can be reached by following the procedure outlined by Ngai et al.[23] Here, the α-relaxation broadening is characterized by the stretching exponent β cor-
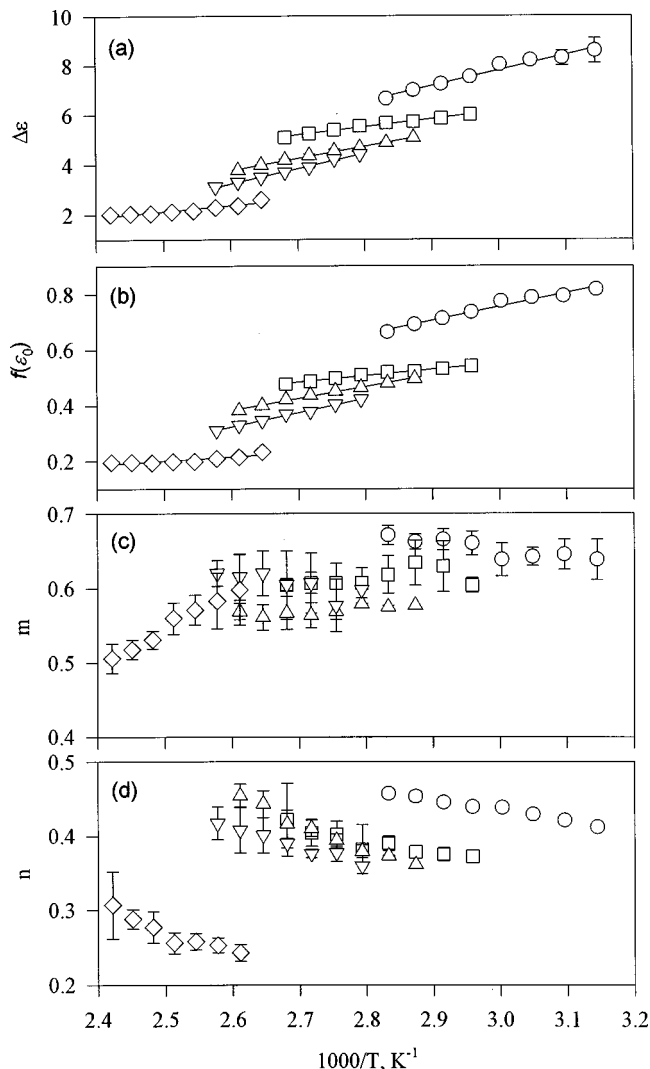

FIG. 5. (a) Dielectric strength, $\Delta\epsilon$, (b) reduced dielectric strength $f(\epsilon_0)$ and scaling parameters, (c) $m = b$, and (d) $n = b \cdot c$ of the α relaxation as a function of the reciprocal temperature for: 100/0○, 75/25□, 60/40△, 43/57▽, and 0/100◇.
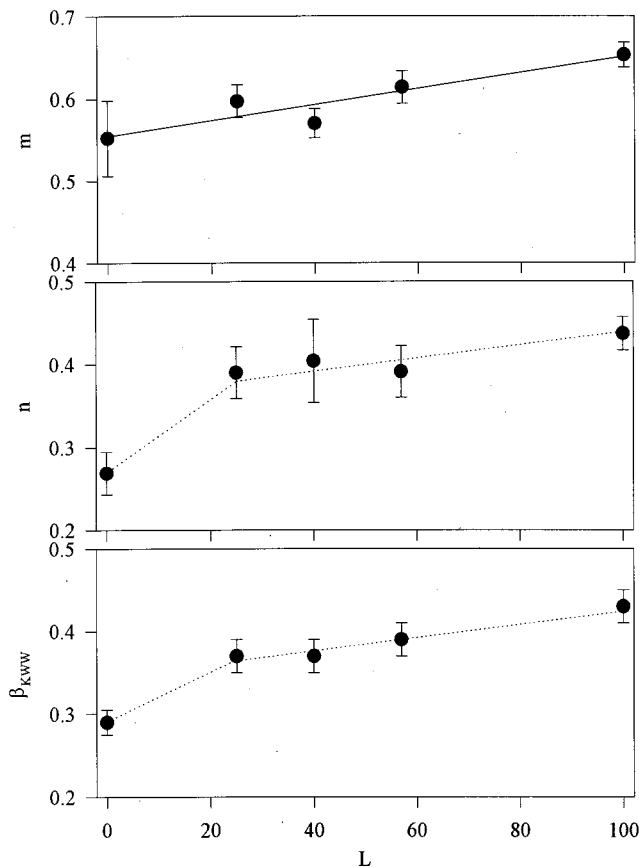

FIG. 6. Scaling parameters $m = b$, $n = b \cdot c$, and β stretching exponent as a function of molar content of the linear component (L). Error bars take account of the temperature dependence of the parameters. Solid lines are guides for the eye.

responding to the Kohlrausch–Williams–Watts (KWW) function which describes the relaxation function in the time domain. As previously described,[16] from the b and c parameter of the HN analysis, we obtained the values of β (Table III) by pure imaginary inverse Laplace transformation and subsequent fitting of the time domain relaxation function to a KWW stretched exponential. This approximation has been shown to be valid provided that $b > 0.4$ and $c > 0.2$.[31] The values of β for the investigated HPN systems (Fig. 6) decrease as the molar ratio of the cross-linked component increases. The coupling model proposed by Ngai *et al.* considers the intermolecular coupling of relaxing species with neighboring nonbonded ones as the main reason for the appearance of a non-Debye behavior.[32,33] The degree of coupling (cooperativity) can be characterized by the experimentally observed β value. According to the coupling model, one may expect a decrease of the β parameter, provided that a strengthening of the intermolecular coupling between the relaxing species occurs. Consequently, we may interpret the observed decrease of β, within this context, as a consequence of the increase of interchain coupling between the relaxing units caused by the additional constraints introduced by the cross-linking.

V. CONCLUSIONS

The specific influence of cross-linking on the α relaxation in polymer networks has been described by studying a series of model heterocyclic polymer networks (HPN) with a well-defined degree of cross-linking and a constant dipolar units concentration. HPN model systems were prepared by simultaneous trimerization of 1,6-hexamethylene diisocyanate (HMDI) and hexyl isocyanate (HI). In these materials the α relaxation depends on network density and shifts toward high temperatures as the cross-link's density increases for high HMDI/HI ratios. Analysis of the α relaxation in terms of the Havriliak–Negami formulation and description of the results in light of the Schönhals–Schlosser phenomenological model, allowed us to conclude that segmental motions above T_g experience an increasing hindrance for both long- and short-scale motions with a systematic cross-linking increase. Evaluation of the temperature dependence of the relaxation time in light of the strong–fragile concept clearly shows that an increase in system fragility occurs as the polymer network develops.

[1] M. Doi, *Introduction to Polymer Physics* (Clarendon, Oxford, 1996).
[2] P. G. de Gennes, *Scaling Concepts in Polymer Physics* (Cornell University Press, Ithaca, NY, 1979).
[3] P. G. de Gennes, J. Chem. Phys. **55**, 572 (1971).
[4] P. G. de Gennes, J. Phys. (Paris) **42**, 735 (1981).
[5] B. D. Fitz and J. Mijovic, Macromolecules **32**, 3518 (1999).
[6] A. R. Kannurpatti and Ch. N. Bowman, Macromolecules **31**, 3311 (1998).
[7] E. Schlosser and A. Schonhals, Colloid Polym. Sci. **267**, 133 (1989).
[8] T. Nicolai, F. Prochazka, and D. Durand, Phys. Rev. Lett. **82**, 863 (1999).
[9] R. Casalini, D. Fioretto, A. Livi, M. Lucchesi, and P. A. Rolla, Phys. Rev. B **56**, 3016 (1997).
[10] J. K. W. Glatz-Reichenbach, L. J. Sorriero, and J. J. Fitzgerald, Macromolecules **27**, 1338 (1994).
[11] A. Bloodworth and A. G. Davies, J. Chem. Soc. **5**, 6858 (1965).
[12] S. Dabi and A. Zilkha, Eur. Polym. J. **17**, 35 (1981).
[13] E. R. Badamshina and S. M. Baturin, Polym. Mater. Sci. Eng. **66**, 142 (1992).
[14] E. R. Badamshina, V. A. Grigor'eva, V. V. Komratova, A. I. Kuzaev, Yu. A. Ol'khov, V. P. Lodygina, G. A. Gorbushina, and S. M. Baturin, Int. J. Polymeric Mater. **19**, 1175 (1993).
[15] E. R. Badamshina, V. A. Grigor'eva, V. V. Komratova, A. I. Kuzaev, and S. M. Baturin, Polym. Sci. USSR **35**, 157 (1993).
[16] T. A. Ezquerra, J. Majszczyk, F. J. Balt-Calleja, E. Lpez-Cabarcos, K. H. Gardner, and B. S. Hsiao, Phys. Rev. B **50**, 6023 (1994).
[17] T. A. Ezquerra, M. Zolotukhin, V. P. Privalko, F. J. Baltá-Calleja, G. Nequlqueo, C. García, J. G. de la Campa, and J. de Abajo, J. Chem. Phys. **110**, 10134 (1999).
[18] S. Havriliak and S. Negami, Polymer **8**, 161 (1967).
[19] K. U. Kirst, F. Kremer, and V. Litvinov, Macromolecules **26**, 975 (1993).
[20] R. Richert and C. A. Angell, J. Chem. Phys. **108**, 9016 (1998).
[21] C. A. Angell, Polymer **38**, 6261 (1997).
[22] C. A. Angell, J. Non-Cryst. Solids **131**, 13 (1991).
[23] C. M. Roland and K. L. Ngai, Macromolecules **25**, 5765 (1992).
[24] R. Böhmer, K. L. Ngai, C. A. Angel, and D. J. Plazek, J. Chem. Phys. **99**, 4201 (1993).
[25] A. Schönhals and E. Schlosser, Colloid Polym. Sci. **267**, 125 (1989).
[26] A. Schönhals, F. Kremer, and E. Schlosser, Phys. Rev. Lett. **67**, 999 (1991).
[27] P. Hedvig, *Dielectric Spectroscopy of Polymers* (Adam Hilger, Bristol, 1977).
[28] R. Díaz-Calleja, E. Riande, and J. San Román, Macromolecules **24**, 264 (1991).
[29] J. C. Coburn and R. H. Boyd, Macromolecules **19**, 2238 (1986).
[30] R. Casalini, A. Livi, P. A. Rolla, G. Levita, and D. Fioretto, Phys. Rev. B **53**, 564 (1996).
[31] F. Alvarez, A. Alegría, and J. Colmenero, Phys. Rev. B **47**, 125 (1993).
[32] K. L. Ngai and C. T. White, Phys. Rev. B **20**, 2475 (1979).
[33] K. L. Ngai, A. K. Rajagopal, and S. Teitler, J. Chem. Phys. **88**, 5086 (1988).